Electronic Supplementary Material (ESI) for Journal of Materials Chemistry A.

Supplementary Information

Holey Amorphous FeCoO Encapsulated Black Phosphorus for Robust Polysulfides Adsorption and Catalytic Conversion in Lithium−Sulfur Batteries

Guodong Zhang[a], Shanshan Wang[a], Xinqian Zeng[b], Xingyun Li,[b] Liangping Xiao[b], Kai Chen[b], Qinhuan Lu[c]， Qingchi Xu*[b], Jian Weng*[a] and Jun Xu*[b,d]

Experimental Section

Materials. Red phosphorus (RP), tin (Sn), and tin iodide (SnI_4) were purchased from Aladdin (Shanghai, China). Tetrabutylammonium hexafluorophosphate (TBAP, 98%) was obtained from Macklin. Cobalt (II) acetate tetrahydrate ($Co(OAc)_2 \cdot 4H_2O$), iron(II) dichloride anhydrous ($FeCl_2$), sodium acetate anhydrous, ethylene glycol, N-methyl-2-pyrrolidone (NMP) and N,N-dimethylformamide (DMF) were purchased from Xilong Chemical Co., Ltd. The lithium plates were purchased from China Energy Co. Ltd. The Celgard 2400 separators (25 μm in thickness) were purchased from Celgard Co. Ltd. All chemicals were used without further purification.

1. Preparation of bulk BP

The bulk BP was obtained by a mineralizing method using RP as a raw material. First, seal RP, Sn, and SnI_4 in a quartz ampoule and vacuum the tube. The quartz ampoule was then placed in the Muffle furnace and heated to 650 °C at a rate of 1.35 °C per minute and maintained at this temperature for 5 hours. After the heating process was finished, the tube was cooled to 500 °C at a rate of 0.33 °C per minute and then cooled naturally to room temperature. The obtained BP crystals were washed with hot toluene and acetone to remove the residual mineralizer. After vacuum drying, they were stored in the glove box for future use.

2. Preparation of BP nanosheets

BP nanosheets were prepared by the typical electrochemical exfoliation method. In short, 100 mg BP crystal was clamped on an electrode as the cathode and platinum sheet as the anode. The electrolyte was 40 mL DMF dissolved with 1.6 g tetrabutylammonium hexafluorophosphate (TBAP). Next, after applying a potential of -10 to -15V to the electrodes by using a DC power supply, BP sheets could be effectively obtained under the embedment of TBA^+ ions. After that, the obtained BP dispersion was washed with DMF solution 7 times to remove the TBAP. BP dispersed in DMF were further ultrasonic in an ice bath for 4 hours to obtain ultra-thin nanosheets and centrifuged at 2000 rpm for 20 min to remove larger bulk materials. Finally, we collected the upper solution and kept it in the refrigerator for further use.

3. Preparation of BP@FeCoO, c-FeCoO and BP@c-FeCoO

BP@FeCoO nanosheets are synthesized by a solvothermal method. Typically, 90 mg of $Co(OAc)_2{\cdot}4H_2O$, 45 mg of $FeCl_2$ and 500 mg of sodium acetate anhydrous were dispersed in 50 mL of ethylene glycol. Then 20 mg of BP nanosheets were mixed with the above solution by sonicating for 30 min. The mixture was then sealed in a 100 mL Teflon-lined stainless-steel autoclave and heated to 200 ^{o}C for 1 hour. After cooling, the product was washed with ethanol three times and dried in vacuum conditions at 60 ^{o}C for 6 hours. c-FeCoO was synthesized at the same conditions without BP. While the BP@c-FeCoO was prepared by the same solvothermal method along with extending the reaction times to 10 h at 220 ^{o}C.

4. Preparation of BP@FeCoO1:2, BP@FeCoO2:1, BP@CoO and BP@FeO

Different amorphous transitional metal (cobalt and/or iron) oxides coated BP were synthesized at the methods with different molar ratios of Co^{2+} and/or Fe^{2+} (1:2, 2:1, 0:1 and 1:0).

5. Preparation of BP@FeCoO 2.0 and BP@FeCoO 0.5

The BP@FeCoO 2.0 was synthesized by the same solvothermal method with 20 mg of BP, 180 mg of $Co(OAc)_2{\cdot}4H_2O$, 90 mg of $FeCl_2$ and 1000 mg of sodium acetate anhydrous. While the BP@FeCoO 0.5 was prepared with 20 mg of BP, 45 mg of $Co(OAc)_2{\cdot}4H_2O$, 22.5mg of $FeCl_2$ and 250 mg of sodium acetate anhydrous.

6. Preparation of BP@FeCoO@S powder

The BP@FeCoO@S composites were prepared according to the classical melt diffusion approach. The as-prepared BP@FeCoO was mixed with sublimed sulfur (the ratio of weight between the hosts and sulfur was 2:8) through adequate grinding in a mortar and then heated at 155 ºC for 12 h in a sealed glass bottle. The procedure of sulfur loading was repeated 3 times to ensure that the sulfur was infiltrated into the BP@FeCoO. Finally, the composites were heated at 160 ºC in an opened glass bottle to remove extra sulfur.

7. Preparation of BP@FeCoO@S electrode

To obtain BP@FeCoO@S electrode, BP@FeCoO@S powder, polyvinylidene fluoride (LA133), and super P (SP) were firstly dispersed in DI-water and ethanol. Then the raw materials were mixed at a mass ratio of 8:1:1 (BP@FeCoO@S: SP. LA133) to acquire uniformly slurry. After stirring for 6 h, the slurry was coated on aluminum foil with a doctor blade and dried in a vacuum oven at 60 °C overnight. After that, the painted aluminum foil was punched to disks with 12 mm in diameter.

8. Material characterization

The atomic force microscope (AFM) images used the Nanoscope Multimode 8 (Bruker, Santa Barbara, USA) to analyze the thickness of the nanosheets. The micrographs of samples were taken using a transmission electron microscope (TEM, JEOL JEM-2100) with the accelerating voltage of 200 kV, high-resolution TEM (HRTEM, TECNAI F-30) with an accelerating voltage of 300 kV. High-energy TEM mapping and energy dispersive X-ray spectra (EDS)-mapping images were conducted on FEI Themis Z equipped with the accelerating voltage of 200 kV. The morphologies were characterized by a scanning electron microscope (SEM, LEO-1530). The X-ray diffraction (XRD, Philips PANalytical X'Pert) equipped with Cu Kα radiation (λ =

1.542 Å) over the 2θ range of 10–80° was used to characterize the lattice structure. X-ray photoelectron spectroscopy (XPS, PHI Quantera SXM) was used to measure the surface components of samples. Then the data were analyzed by using the Xpspeak41 software. The EPR sample was prepared in airtight EPR tubes (4 mm LPV 250 mm EPR sample tube) purchased from Wilmad LabGlass. Electron paramagnetic resonance (EPR) spectra were obtained on a Bruker EMXplus EPR spectrometer. The freshly made sample tube was inserted into the measurement chamber and then put through the temperature of 100 K.

9. Electrochemical Measurements

The 2032 coin cells were assembled in an Ar-filled glove box (O_2, H_2O < 0.1 ppm) with an electrolyte of 1.0 M LiTFSI and 0.2 M $LiNO_3$ in DOL/DME (v:v,1:1). CT2001A tester (LAND Electronic Co. Ltd., Wuhan) was applied to record the electrochemical behavior in Li−S CR2032 type coin cells. The electrochemical impedance spectroscopy was measured in the frequency range from 100 kHz to 0.1 Hz with 5 mV amplitude. The conductivity measurements were performed using the van der Pauw method with the RTS-9 four-point probes resistivity measurement system.[1] The powder was pressed into a thin circular sheet with a diameter of 8 mm and a thickness of 0.5-1 mm by a mold. The four-probe contacts are placed on a thin wafer and the probe connection is manually changed for measurement.

10. Lithium sulfide adsorption test

Li_2S_6 solution was prepared by dissolving Li_2S and S with a molar ratio of 1:5 into a mixed solution containing DOL and DME (1:1 by volume) with subsequently stir in an Ar-filled glove box at 80 °C. The same mass (10 mg) of BP@FeCoO, BP@c-FeCoO, c-

FeCoO and BP were added into the solution with 10 mM Li_2S_6, dividedly. The solution was standing for some time to evaluate the adsorption capabilities of BP@FeCoO, BP@c-FeCoO, c-FeCoO and BP.

11. Symmetrical cell assembly and measurements

The symmetrical cells were assembled using active material (BP@FeCoO, BP@c-FeCoO, c-FeCoO or BP) both as working and counter electrodes. The electrolyte contains 0.2 M Li_2S_6 and 1 M bis(trifluoroethanesulfony)imide lithium (LiTFSI) dissolved in the DOL/DME mixed solution (1:1 by volume). The CV tests of the symmetrical cells were measured in a voltage range from -1 to 1 V with a scan rate of 10 mV s^{-1}.

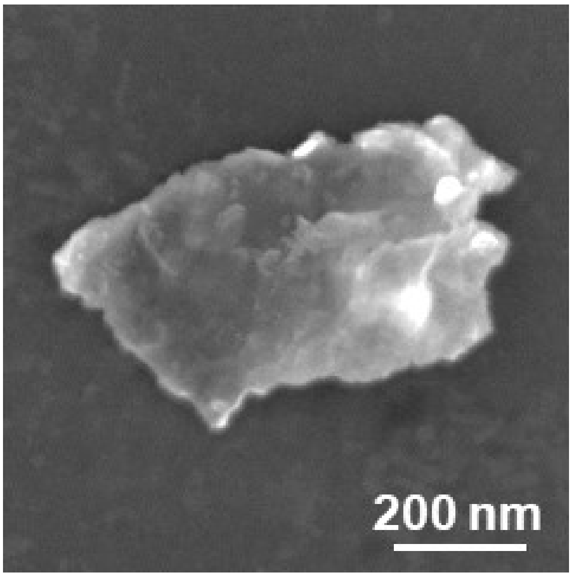

Fig. S1. SEM image of BP@FeCoO.

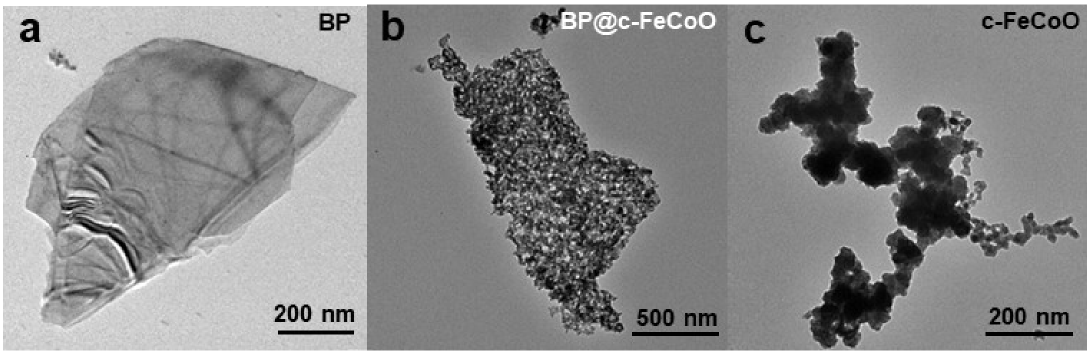

Fig. S2. TEM images of a) BP, b) BP@c-FeCoO and c) c-FeCoO.

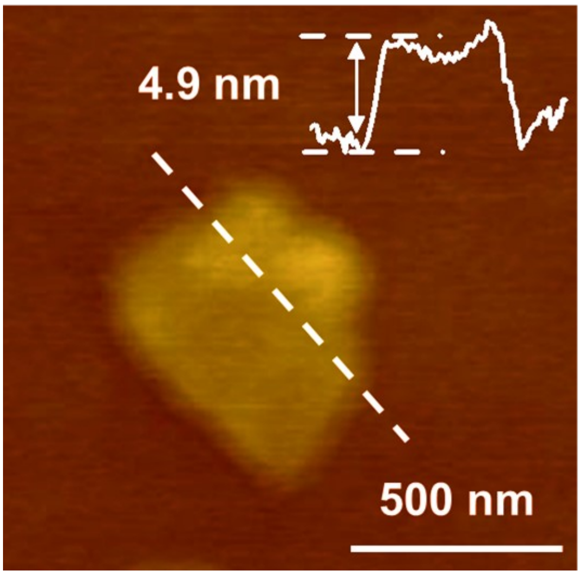

Fig. S3. AFM image of the BP nanosheet.

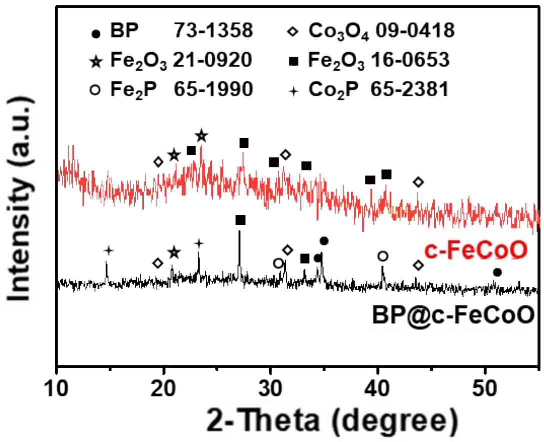

Fig. S4. XRD patterns of BP@c-FeCoO and c-FeCoO.

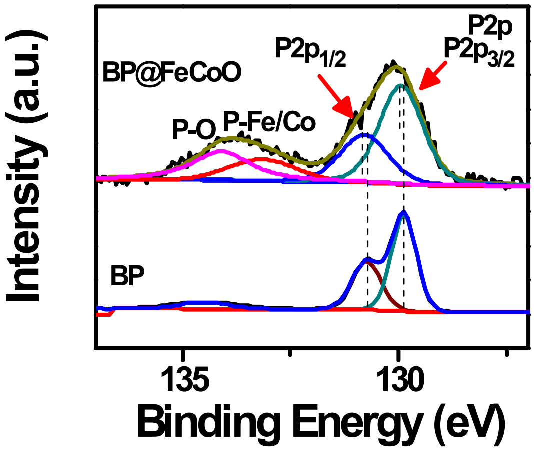

Fig. S5. High-resolution XPS spectra of P 2p for BP@FeCoO and BP.

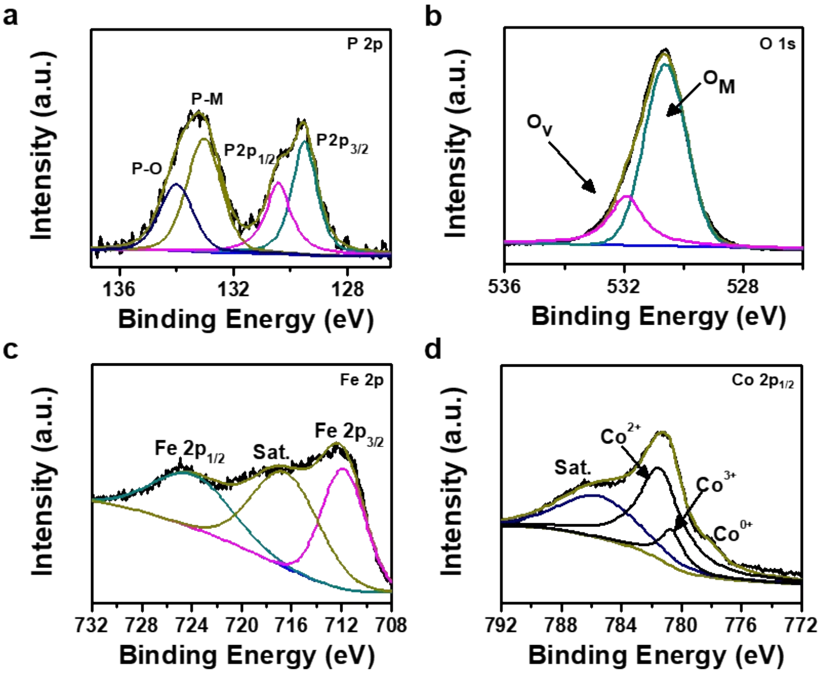

Fig. S6. High-resolution XPS spectra of P 2p, O 1s, Fe 2p and Co 2p$_{1/2}$ for BP@c-FeCoO.

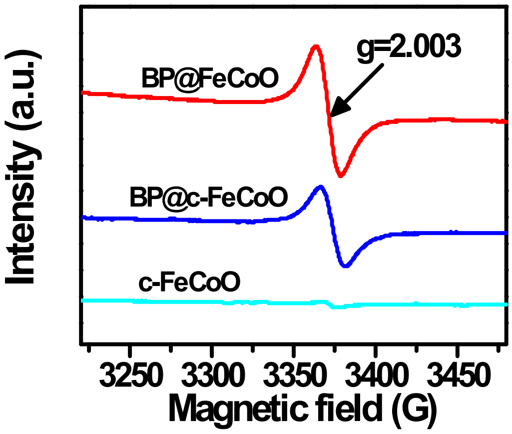

Fig. S7. Electron paramagnetic resonance (EPR) spectra of BP@FeCoO, BP@c-FeCoO, c-FeCoO.

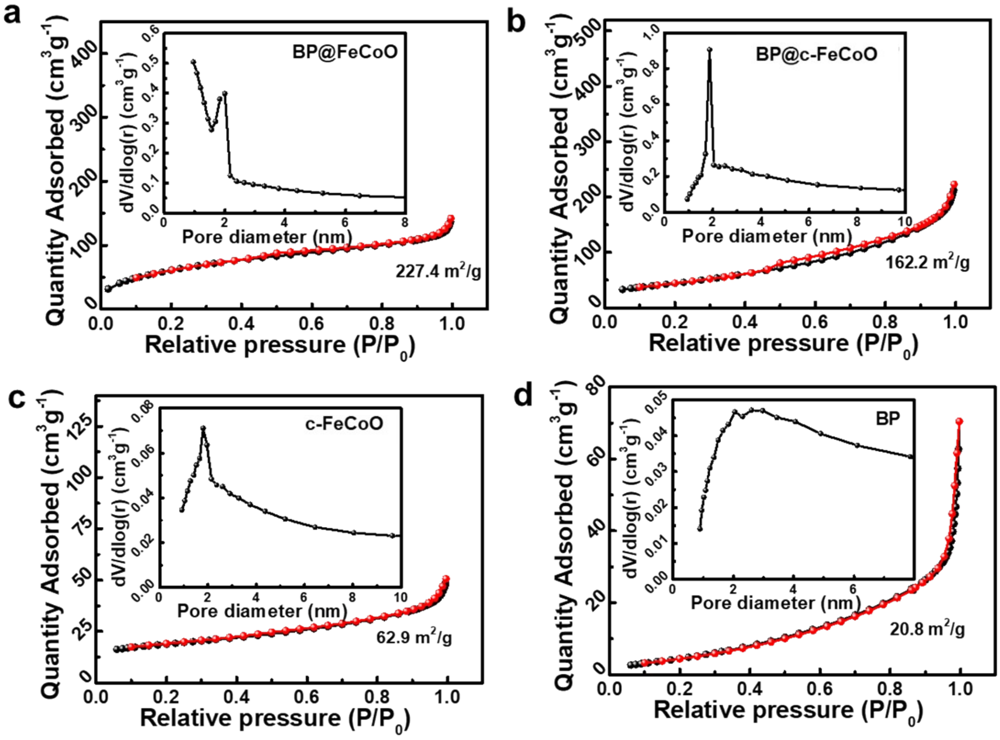

Fig. S8. N_2 adsorption-desorption isotherms of a) BP@FeCoO, b) BP@c-FeCoO, c) c-FeCoO and d) BP, the corresponding pore size distribution graphs are shown inset.

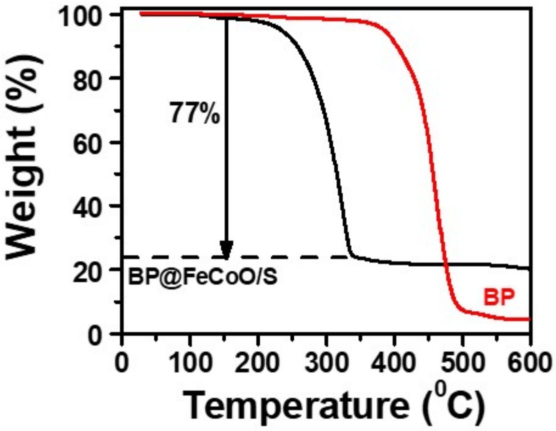

Fig. S9. The thermogravimetric analysis (TGA) curves for BP@FeCoO@S and BP.

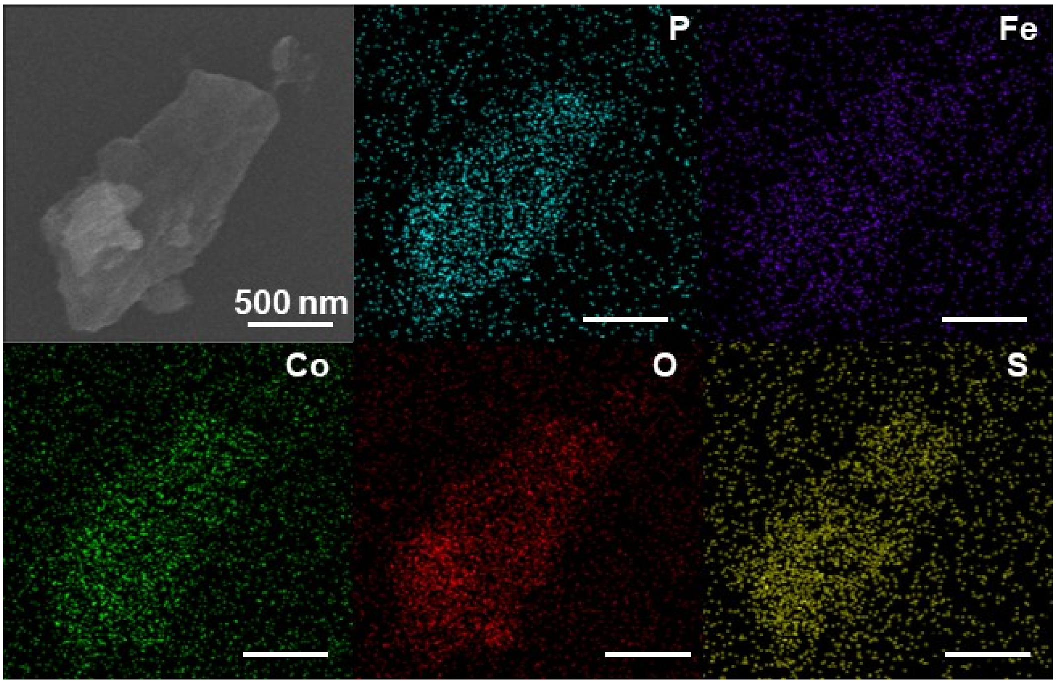

Fig. S10. SEM images for BP@FeCoO@S cathode and the corresponding EDS elemental mappings.

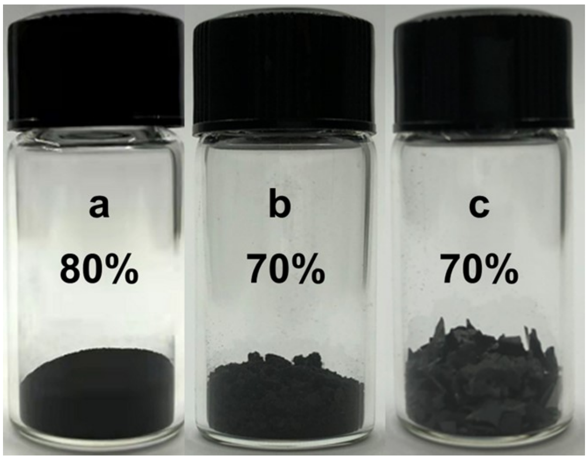

Fig. S11. Photographs of a) BP@FeCoO with 80% sulfur loading, b-c) 70% sulfur loading of b) BP@c-FeCoO and c) c-FeCoO, respectively.

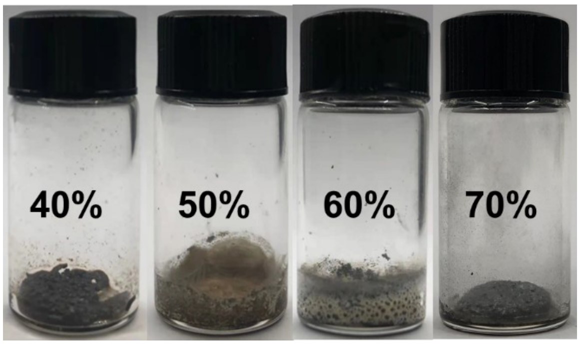

Fig. S12. Photographs of BP after loading with 40%, 50%, 60% and 70% amount of sulfur, respectively.

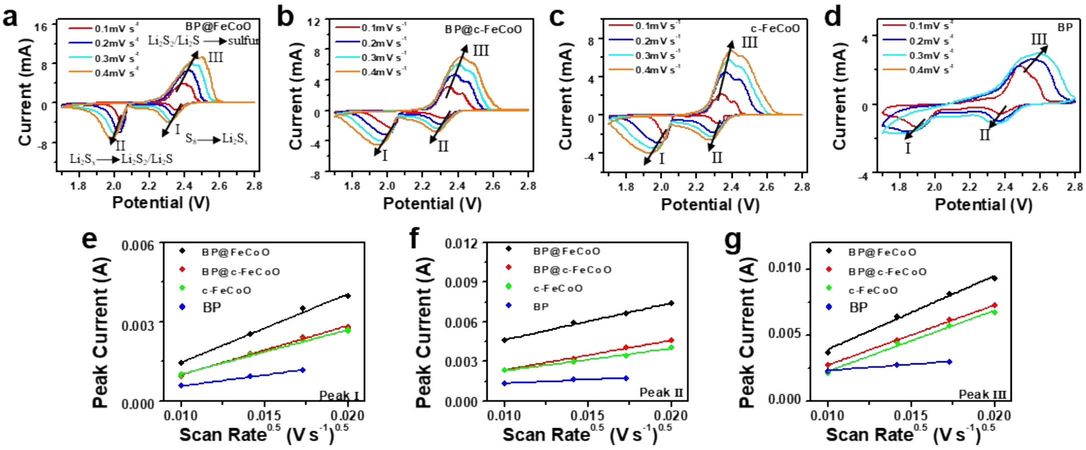

Fig. S13. CV curves of the a) BP@FeCoO, b) BP@c-FeCoO, c) c-FeCoO and d) BP at different scan rates in the voltage range of 1.7-2.8V. Linear fits of CV peak current depend on the square root of the scan rates in e) peak I, f) peak II, and g) peak III.

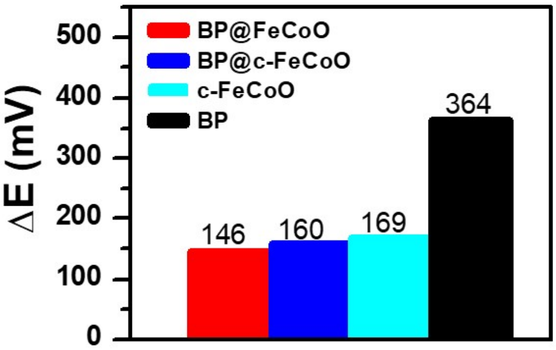

Fig. S14. The polarization potential of Li−S batteries with different electrodes.

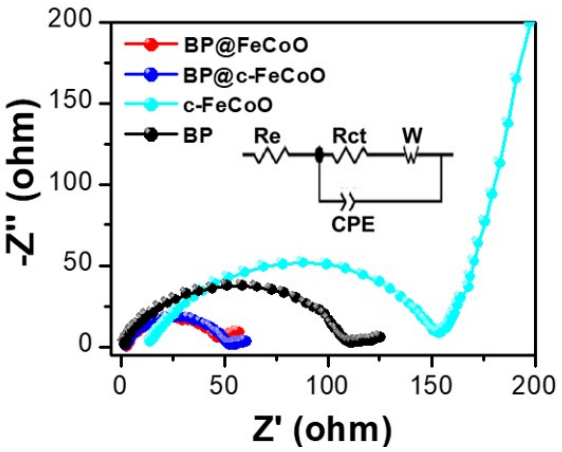

Fig. S15. Nyquist plots of BP@FeCoO, BP@c-FeCoO, c-FeCoO and BP.

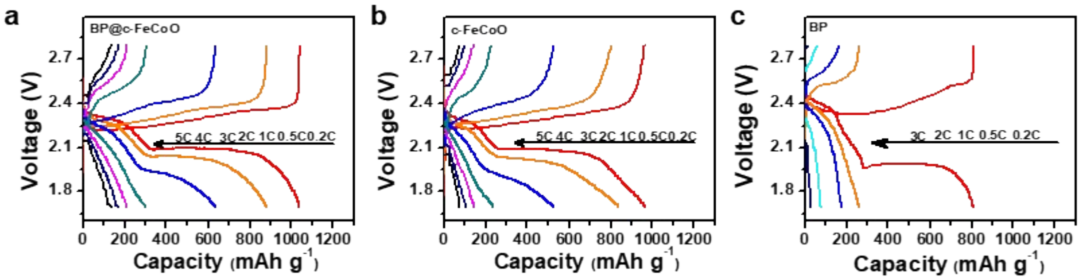

Fig. S16. Galvanostatic charge-discharge profiles of a) BP@c-FeCoO/S, b) c-FeCoO/S, and c) BP/S electrodes at current rates from 0.2 to 5 C.

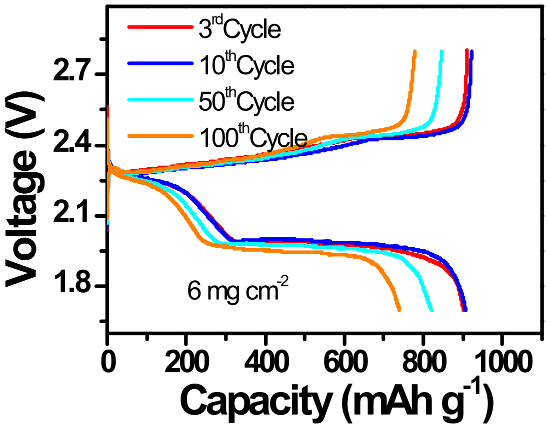

Fig. S17. Charge/discharge curves at 0.2 C with sulfur loadings of 6 mg cm^{-2}.

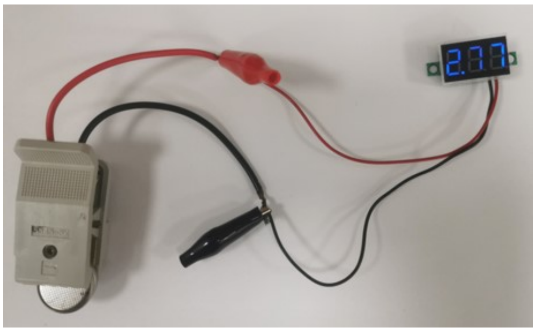

Fig. S18. Digital photograph of LED illuminated by Li-S battery based on the BP@FeCoO electrode.

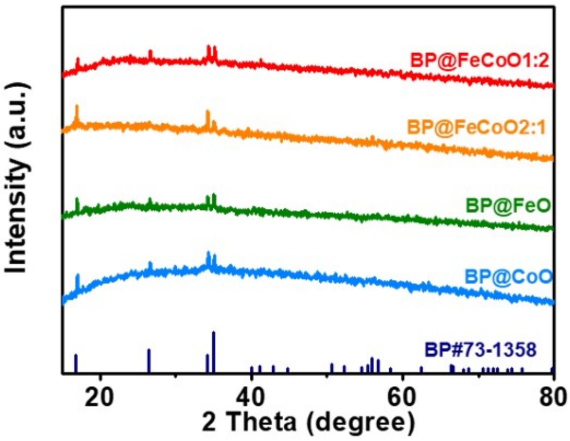

Fig. S19. XRD patterns of BP@FeCoO1:2, BP@FeCoO2:1, BP@CoO, and BP@FeO.

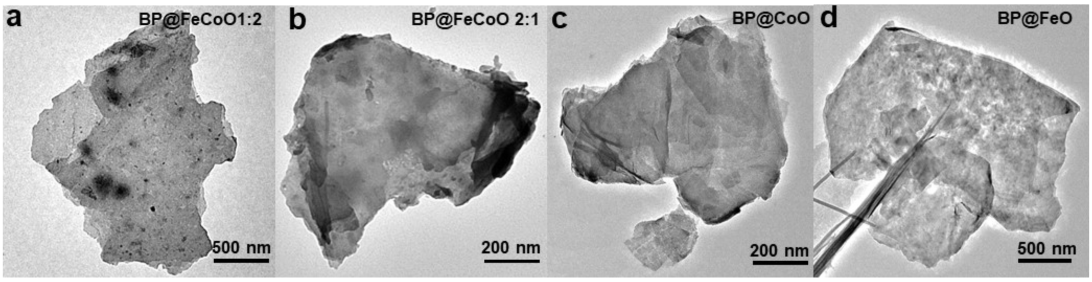

Fig. S20. TEM images of a) BP@FeCoO1:2, b) BP@FeCoO2:1, c) BP@CoO, and d) BP@FeO.

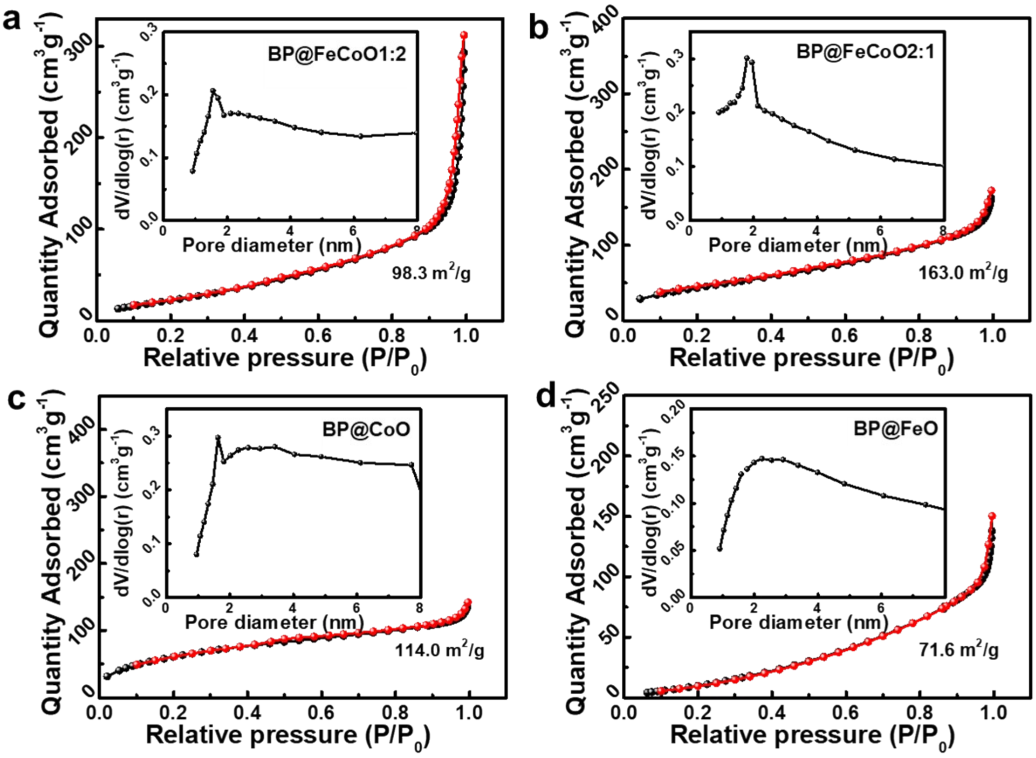

Fig. S21. N_2 adsorption-desorption isotherms of a) BP@FeCoO1:2, b) BP@FeCoO2:1, c) BP@CoO and d) BP@FeO, the corresponding pore size distribution graphs are shown inset.

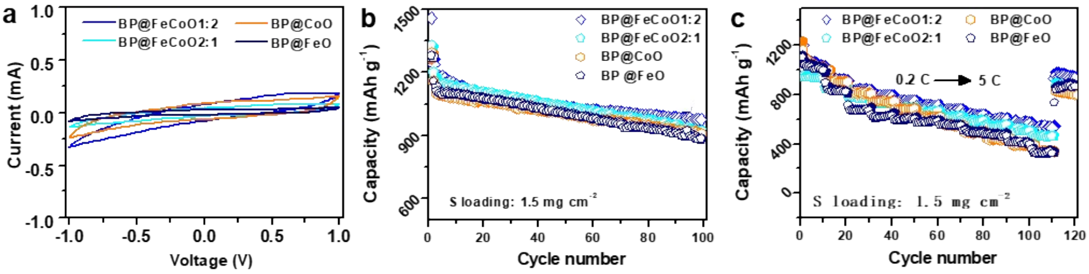

Fig. S22. Electrochemical performance of BP@FeCoO1:2, BP@FeCoO2:1, BP@CoO and BP@FeO, respectively. a) CV curves of symmetrical cells at a scan rate of 10 mV^{-1}. b) Cycling performance at 0.2C. c) Rate performance.

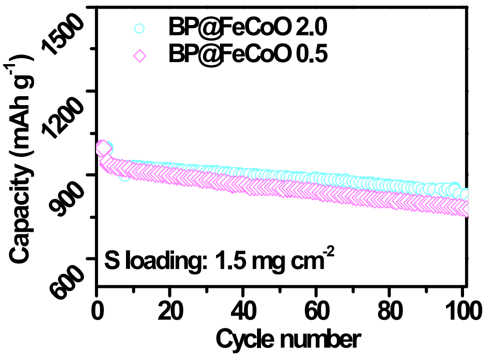

Fig. S23. Electrochemical performance of BP@FeCoO 2.0 and BP@FeCoO 0.5 at 0.2C.

Table S1. Electric conductivities of BP@FeCoO, BP@c-FeCoO, c-FeCoO, and BP.

Parameters	Electric conductivities (S cm^{-1})
BP@FeCoO	3.57×10^{-3}
BP@c-FeCoO	1.29×10^{-4}
c-FeCoO	3.19×10^{-4}
BP	1.52×10^{-3}

Table S2. Li^+ diffusion coefficients of the BP@c-FeCoO/S, c-FeCoO/S and BP/S electrodes.

Parameters	D_{Li^+} at peak I (cm^2 s^{-1})	D_{Li^+} at peak II (cm^2 s^{-1})	D_{Li^+} at peak III (cm^2 s^{-1})
BP@c-FeCoO/S	7.05×10^{-9}	4.14×10^{-8}	5.76×10^{-8}
c-FeCoO/S	7.57×10^{-9}	4.12×10^{-8}	3.38×10^{-8}
BP/S	2.48×10^{-9}	1.31×10^{-8}	4.11×10^{-8}

Table S3. Comparisons of the electrochemical performance of Li-S batteries with different catalysts.

Sample	Sulfur content (wt%)	Sulfur loading (mg cm^{-2})	Reversible capacity (mAh g^{-1})	Fading rate per cycle (%)	Ref.
Phosphorene /CNF/Li_2S_6	-	3.3	660 (1C, 500 cycles)	0.053	S2[2]
BP Modified Separator	80	1.5-2.0	800 (0.2C, 100 cycles)	0.140	S3[3]
PCNF/S/BPQD	-	2.0	589 (2C, 1000 cycles)	0.027	S4[4]
EBP/EGr@S	75	-	1024 (0.2C, 100 cycles)	0.170	S5[5]
CoFeP@CN/S	70	1.0	606 (3C, 700 cycles)	0.014	S6[6]
$CoFe_2O_4$/S	70	2.0	600(2C, 600 cycles)	0.030	S7[7]
$CoFe_2O_4$@C cathode	74.3	-	557 (1C, 500 cycles)	0.063	S8[8]
$CoFe_2O_4$@ PANI	74.6	-	582.6 (2C, 500 cycles)	0.065	S9[9]
$NiMoO_4$@NSCC/S	-	2.0	1153.7 (0.2C, 80 cycles)	1.712	S10[10]
BP@FeCoO/S	**78**	**1.5-2.5**	**1060.5 (0.2C, 100 cycles)** **703.6 (1C, 500 cycles)**	**0.085** **0.04**	**This work**

Table S4. The mass ratios of BP to FeCoO in different BP@FeCoO samples

Sample	**ICP-OES (wt%)**	
	BP	**FeCoO**
BP@FeCoO 0.5	27.0	73.0
BP@FeCoO	19.1	80.9
BP@FeCoO 2.0	11.1	88.9

References

1. D. Sheberla, L. Sun, M. A. Blood-Forsythe, S. l. Er, C. R. Wade, C. K. Brozek, A. n. Aspuru-Guzik, M. Dincă, *J. Am. Chem. Soc.* 2014, **136**, 8859-8862.
2. L. Lu, C. Long, S. Mukherjee, G. Jian, N. Koratkar, *Adv. Mater.* 2016, **29**, 1602734.
3. J. Sun, Y. Sun, M. Pasta, G. Zhou, Y. Li, W. Liu, F. Xiong, Y. Cui, *Adv. Mater.* 2016, **28**, 9797-9803.
4. Z. L. Xu, S. Lin, N. Onofrio, L. Zhou, F. Shi, W. Lu, K. Kang, Q. Zhang, S. Lau, *Nat. Commun.* 2018, **9,** 1-11.
5. J. Zhou, T. Wu, Y. Pan, J. Zhu, X. Chen, C. Peng, C. Shu, L. Kong, W. Tang, S. Chou, *Adv. Funct. Mater.* 2021, 2106966.
6. C. Zhang, R. Du, J. J. Biendicho, M. Yi, K. Xiao, D. Yang, T. Zhang, X. Wang, J. Arbiol, J. Llorca, *Adv. Energy Mater.* 2021, **11**, 2100432.
7. D.-R. Deng, X.-Y. Cui, X.-X. Fan, J.-Q. Zheng, X.-H. Fan, Q.-H. Wu, M.-S. Zheng, Q.-F. Dong, Fuels, *Sustainable Energy Fuels* 2021, **5**, 4284-4288.
8. L.-L. Gu, J. Gao, C. Wang, S.-Y. Qiu, K.-X. Wang, X.-T. Gao, K.-N. Sun, P.-J. Zuo, X.-D. J. Zhu, *J. Mater. Chem. A* 2020, **8**, 20604-20611.
9. L.-L. Gu, C. Wang, S.-Y. Qiu, K.-X. Wang, X.-T. Gao, P.-J. Zuo, K.-N. Sun, X.-D. Zhu, *Electrochim. Acta* 2021, **390**, 138873.
10. T. Sun, X. Zhao, B. Li, H. Shu, L. Luo, W. Xia, M. Chen, P. Zeng, X. Yang, P. Gao, *Adv. Funct. Mater.* 2021, 2101285.